PNAS RESEARCH ARTICLE | MEDICAL SCIENCES OPEN ACCESS

Early expression of mature αβ TCR in CD4⁻CD8⁻ T cell progenitors enables MHC to drive development of T-ALL bearing NOTCH mutations

Kimberly G. Laffey[a], Robert J. Stiles[b], Melissa J. Ludescher[b], Tessa R. Davis[b], Shariq S. Khwaja[b], Richard J. Bram[b,c], Peter J. Wettstein[b,d], Venkataraman Ramachandran[e], Christopher A. Parks[b], Edwin E. Reyes[b], Alejandro Ferrer[b], Jenna M. Canfield[a], Cory E. Johnson[f], Richard D. Hammer[f,g], Diana Gil[a,e,h], and Adam G. Schrum[a,e,h,1]

Edited by Irving Weissman, Stanford University, Stanford, CA; received October 8, 2021; accepted April 19, 2022

During normal T cell development in mouse and human, a low-frequency population of immature CD4⁻CD8⁻ double-negative (DN) thymocytes expresses early, mature αβ T cell antigen receptor (TCR). We report that these early αβ TCR+ DN (EADN) cells are DN3b-DN4 stage and require CD3δ but not major histocompatibility complex (MHC) for their generation/detection. When MHC - is present, however, EADN cells can respond to it, displaying a degree of coreceptor-independent MHC reactivity not typical of mature, conventional αβ T cells. We found these data to be connected with observations that EADN cells were susceptible to T cell acute lymphoblastic leukemia (T-ALL) transformation in both humans and mice. Using the OT-1 TCR transgenic system to model EADN-stage αβ TCR expression, we found that EADN leukemogenesis required MHC to induce development of T-ALL bearing NOTCH1 mutations. This leukemia-driving MHC requirement could be lost, however, upon passaging the tumors in vivo, even when matching MHC was continuously present in recipient animals and on the tumor cells themselves. These data demonstrate that MHC:TCR signaling can be required to initiate a cancer phenotype from an understudied developmental state that appears to be represented in the mouse and human disease spectrum.

TCR | T-ALL | NOTCH | MHC | leukemia

Significance

T cell development and immune responses are directed by major histocompatibility complex:T cell antigen receptor (MHC:TCR) signaling, but aberrant signals can cause T cell tumors to form. We show that in mice and humans, a low-frequency progenitor cell population expresses early αβ TCR while coreceptor double-negative (EADN), and these EADN cells can transform to thymic leukemia. Mouse models showed that EADN cells did not require MHC to develop but when presented with MHC they could respond with high sensitivity. Transformation to leukemia occurred and required MHC, although with extended tumor growth this requirement could be lost. Thus, MHC:TCR signaling can initiate a leukemia phenotype from an understudied developmental state that appears to be represented in the mouse and human disease spectrum.

T cell acute lymphoblastic leukemia (T-ALL) is an aggressive hematologic malignancy arising from transformed immature T cell precursors (1). It represents ∼15% of pediatric and ∼25% of adult ALLs (2). Identification of subgroups with varied biological features, including overall relapse risk and responses to standard therapies, has allowed stratification of patients to the most appropriate therapeutic regimens that maximize efficacy, and has led to generally improved survival. However, prognosis remains poor for patients with treatment-refractory primary disease or relapse (3, 4). Clinical T-ALL can show inter- and intrapatient heterogeneity in the differentiation stage of tumor cells, implying that multiple pathways of cancer development exist (1, 5). Despite the heterogeneity, a unifying oncogenic network hub required for most or all T-ALL in humans and mice is hyperactivated (often mutated) NOTCH (6). Among the best understood causal drivers is developmentally early CD3 signaling at the pre-T cell antigen receptor (TCR)/γδTCR lineage bifurcation checkpoint, without a role for major histocompatibility complex (MHC)-based ligand (7–9). In contrast, a requirement for MHC and mature αβTCR to drive thymic leukemogenesis, resulting in mutant NOTCH-bearing tumors, has not been previously demonstrated.

This makes sense based on the known relationship between T-ALL and T cell development. While there is overlap in NOTCH and developmentally early CD3 signals, cessation of NOTCH prior to MHC-restricted positive/negative selection signals mediated by αβTCR largely prevents simultaneous activity of the two receptors. Most conventional thymocytes rearrange first TCRβ and later TCRα loci in separate, ordered developmental stages. NOTCH signaling is required for early CD4⁻CD8⁻ double negative (DN) thymocyte development (10) while rearrangement of TCRβ and pre-TCR expression mediate β-selection, clonal expansion, and advancement to CD4⁺CD8⁺ double-positive (DP) stage (11). NOTCH signaling is then turned off (12), while DP thymocytes rearrange TCRα, express mature αβTCR, and test self-peptide-MHC reactivity in positive/negative selection (13).

However, outside of this well-described sequence of events, a low-frequency, natural subset of DN thymocytes was once shown to rearrange and prematurely express the full αβTCR in wild-type mice (14). The cells were first detected in pre-Tα$^{-/-}$ mice,

Author contributions: K.G.L. and A.G.S. designed research; K.G.L., R.J.S., M.J.L., T.R.D., S.S.K., P.J.W., C.A.P., E.E.R., A.F., J.M.C., C.E.J., R.D.H., and A.G.S. performed research; V.R. and R.D.H. contributed new reagents/analytic tools; K.G.L., T.R.D., S.S.K., R.J.B., P.J.W., R.D.H., D.G., and A.G.S. analyzed data; K.G.L. and A.G.S. wrote the paper; D.G. provided funding acquisition; and A.G.S. provided funding acquisition and supervision.

The authors declare no competing interest.

This article is a PNAS Direct Submission.

[1]To whom correspondence may be addressed. Email: schruma@health.missouri.edu.

This article contains supporting information online at http://www.pnas.org/lookup/suppl/doi:10.1073/pnas.2118529119/-/DCSupplemental.

Published June 29, 2022.

where early TCRα replaced pre-Tα to provide β-selection signaling to generate DP cells. Conventional αβ T cell development potential was retained as proven in positive selection assays, but subsequent to the initial report little information on biological roles for these cells has followed. While pursuing developmental stages and signals in T-ALL leukemogenesis, we found that early αβTCR-expressing DN (EADN) cells can be generated in mouse and human thymus at a similar rate, and they are susceptible to T-ALL transformation in both species. We present a mouse model in which EADN oncogenesis requires MHC to drive development of T-ALL bearing NOTCH-mutations, highlighting a novel developmental state with unique signaling rules for a cancer phenotype that appears to be represented in the clinical, human disease spectrum.

Results

EADN Thymocytes Exist Naturally in Mouse and Human. To determine if some immature mouse DN thymocytes express surface αβTCR as previously reported (14), we used flow cytometry to gate $CD4^-$ $CD8\alpha^-$ DN thymocytes that were negative for γδTCR, negative for binding the natural killer (NK)-T cell ligand αGalCer analog (PBS57) presented in CD1d, and negative for other markers, NK1.1 and CD122 (Fig. 1*A*, *Left*). Because pre-Tα:TCRβ surface complexes are not detected by standard flow cytometry methods (15) surface TCRβ level was used as a readout for αβTCR, an assumption previously validated using pre-$T\alpha^{-/-}$ mice (14), and further validated ahead. We observed that most gated DN thymocytes were negative for surface TCRβ detection, while a small fraction was positive to a full level defined by mature T cells (box gates, Fig. 1*A*, *Right*). Pooling the few available anti-TCRα monoclonal antibodies (mAbs) (Fig. 1*A*, *Right*, *y* axis), we observed that surface TCRβ expression occurred to the same level whether or not cells expressed these Vα's, consistent with the expectation that Vα-pool-negative cells would be positive for other Vα's (Fig. 1*A*, *Right*). We conclude that some αβ DN thymocytes, which are not in known unconventional marker-defined subsets, express full-level surface TCR, representing ∼1% of DN thymocytes, or ∼0.01% of total thymocytes in mice.

Human pediatric thymocytes were assessed by gating $CD4^-$ $CD8\alpha^-$ DN cells that were negative for γδTCR and NK marker CD56 (Fig. 1*B*, *Left* and *Middle*). To a level defined by mature T cells (Fig. 1*B*, *Right*, offset), mAb IP26 detected surface αβTCR expression in ∼0.4% of gated DN thymocytes, or ∼0.01% of total thymocytes (Fig. 1*B*, *Right*). We conclude that EADN thymocytes can be present in similar, naturally low frequencies in both human and mouse species.

To further assess specificity and the requirement of MHC for development, we compared EADN cells detected from wild-type mice with those lacking CD3δ, MHC, or both. As expected, $CD3\delta^{-/-}$ mice produced DN and DP thymocytes and γδ T cells, indicative of functional pre-TCR and γδTCR (16–18), but the knockout blocked αβTCR/CD3 surface expression and detection of EADN cells (Fig. 1*C*). We conclude that surface αβTCR/CD3 expression is required for EADN generation/detection. In contrast, mice lacking MHC classes I and II produced EADN cells in a CD3δ-dependent manner similar to wild-type (Fig. 1*C*). We conclude that generation of EADN cells is independent of MHC-mediated positive selection.

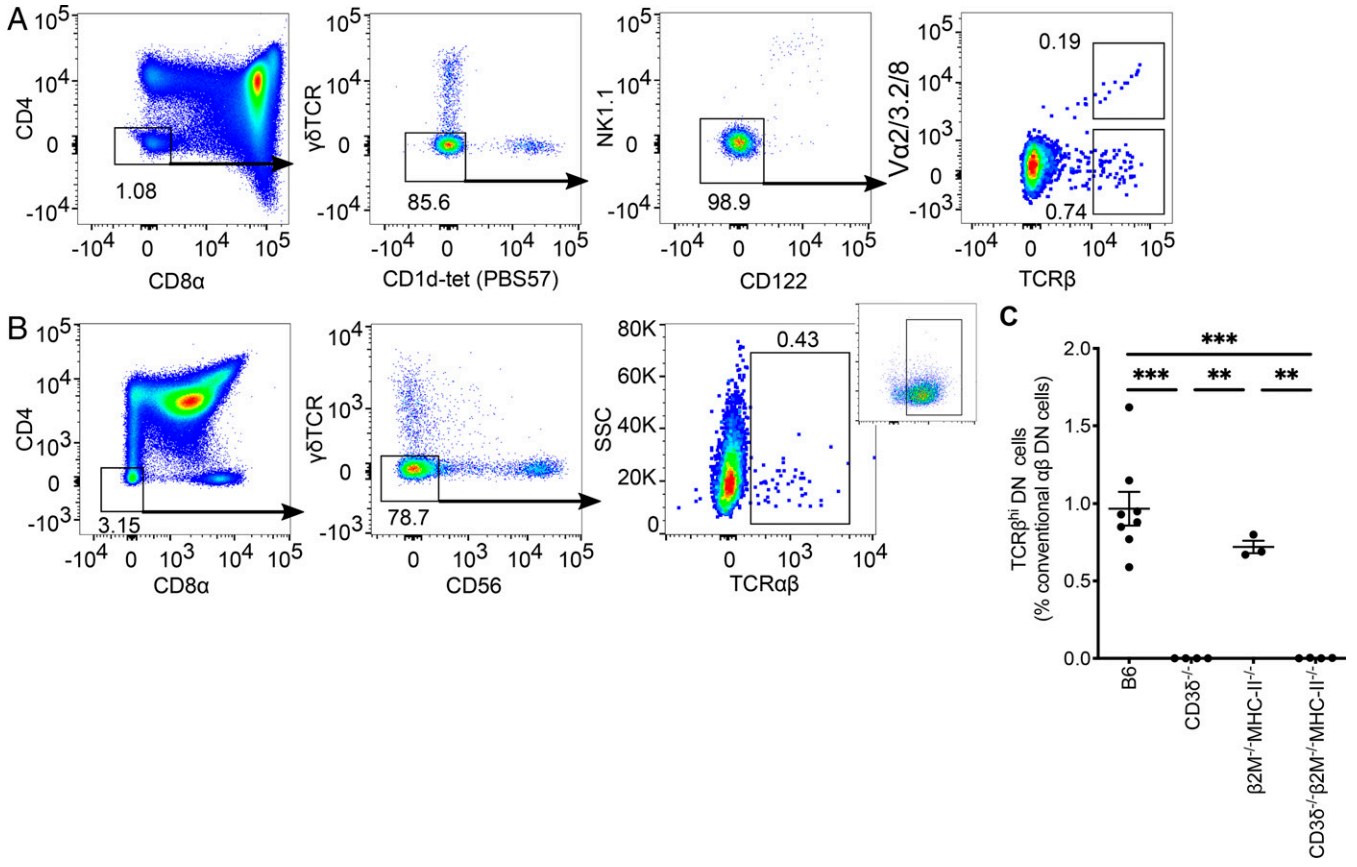

Fig. 1. EADN thymocytes exist naturally in mouse and human. Flow cytometry analysis of thymocytes used to identify EADN cells in (*A*) B6 murine thymus and (*B*) human thymus, where the right-most offset panel represents TCRβ x Side Scatter for CD8 single-positive thymocytes used to identify mature TCRβ surface level. Numbers represent % cells in the gate. (*C*) Quantification of EADN cells in mice with different genetic lesions affecting T cell generation. One-way ANOVA with Tukey's posttest, $^{**}P < 0.01$ $^{***}P < 0.001$.

Wild-Type and OT-1 TCR Transgenic EADN Cell Development and Response to MHC. We observed that wild-type mouse EADN cells appear in the progression of DN3 to DN4 (Fig. 2*A*, *Top*). TCR transgenic OT-1 thymocytes were also found to reach full surface TCR expression closely approximating the EADN stage (*SI Appendix*, Fig. S1*A*) of DN3-DN4 (Fig. 2*A*, *Bottom*). Analogous to the DN3-4 stage of murine EADN cells, human EADN cells mainly exhibited a post-β-selection DN surface phenotype being $CD7^+$ $CD5^+$, up-regulating CD1a (19, 20) and CD28 (21) while down-regulating CD34 (22) (Fig. 2*B*). Also in common with wild-type, OT-1 EADN cell percentages were similar in mice sufficient or deficient in MHC class I, the positive selection MHC for OT-1 (23, 24) (*SI Appendix*, Fig. S1*B*). We conclude that EADN generation was evident at DN3-4 stage and independent of the MHC-based positive selection step required of conventional, mature αβ T cells.

Although MHC was not required for EADN generation, we wished to determine if EADN cells could respond to MHC. First, we observed higher Nur77 expression in EADN cells from wild-type compared to MHC knockout mice (Fig. 2*C*), where Nur77 expression is a common readout downstream of TCR signaling (24). Second, OT-1.$RAG2^{-/-}$.$\beta2M^{-/-}$ fetal thymi were cultured for 24 h in the presence of exogenously added β2-microglobulin (β2M) plus peptide ligands of varying strength for OT-1 stimulation (25, 26). EADN cells from cultured fetal thymi exhibited greater CD69 expression in response to SIINFEKL (OVA) than weaker peptide, Q4H7, and non-OT-1-reactive peptide, FARL (Fig. 2*D*). We conclude that even though surface coreceptor levels are not detected (DN stage), EADN thymocytes can respond to MHC.

To further assess the maturation state of EADN cells, extensive surface phenotyping by multiparametric flow cytometry and spanning-tree progression analysis of density-normalized events (SPADE) was performed. SPADE corroborated that wild-type EADN cells cluster separately from conventional DN2, DN3a, DN3b, and DN4 subsets, and are also distinct from unconventional DN subsets including intestinal intraepithelial lymphocyte precursors, NK-T cells, and γδ T cells (Fig. 2*E*). We conclude that EADN cells can be separated from other immature subsets by surface markers and can be separated from conventional αβ DN developmental stages by αβTCR/CD3 surface expression level. Similar to the data shown for human EADN cells above, mouse EADN cells expressed high CD28 indicating they were at post-β-selection (27) DN3b-DN4 stage (*SI Appendix*, Fig. S2*A*). Finally, we observed that most of the EADN cell population expressed markers of immaturity including high CD24 (*SI Appendix*, Fig. S2 *B* and *C*) and low CD127 (*SI Appendix*, Fig. S2 *D* and *E*), in contrast to mature, peripheral $\alpha\beta TCR^+$ DN T cells, suggesting that the present observations were not dominated by mature, peripheral $\alpha\beta TCR^+$ DN T cells that could recirculate in these thymi (28). We conclude that most EADN thymocytes in the present study displayed an immature thymocyte profile based on DN subset analysis, MHC-independence, and progenitor marker expression.

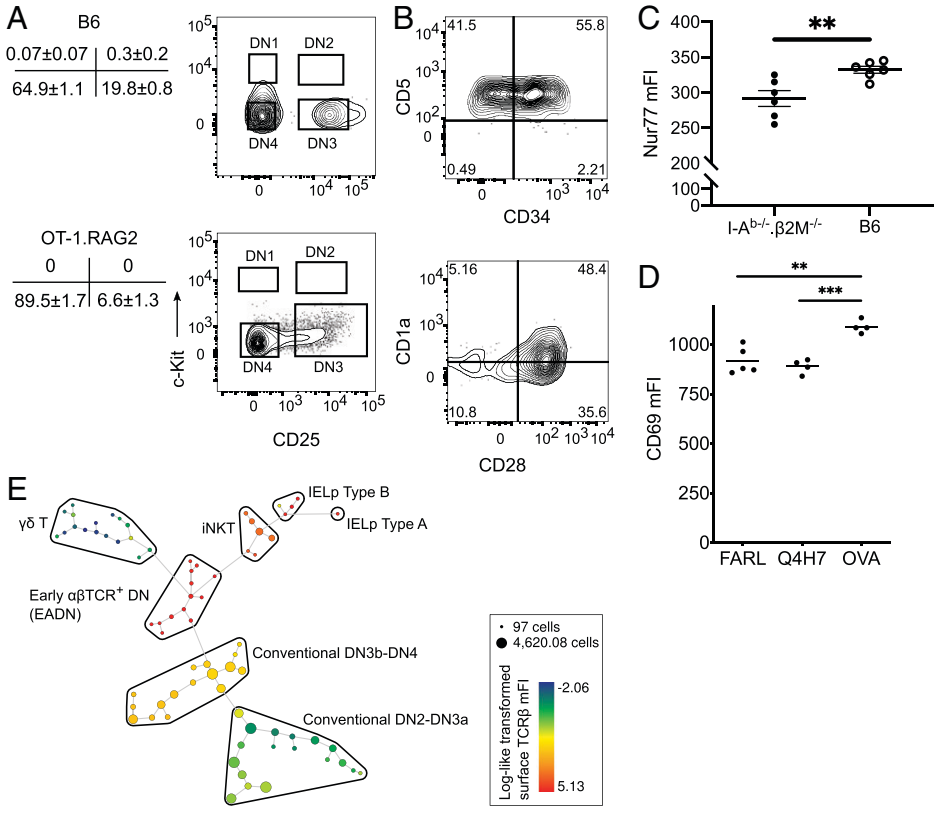

Fig. 2. OT-1 TCR transgenic system provides a model for EADN cell development and response to MHC. (*A*) Representative flow cytometry analysis of surface CD25 and c-Kit expression from wild-type B6 and OT-1 thymocytes gated on $CD4^-CD8a^-$ DN, EADN cells. Average frequencies of each subset from 4 mice are presented with SEM. (*B*) Flow cytometry analysis for surface expression of CD34, CD5, CD1a, and CD28 when gating on human EADN cells. After gating out non-T lineage cells, EADN cells are identified as $CD4^-$ $CD8a^-$ $CD45^{dim}$ $CD7^+$ $\alpha\beta TCR^+$. Numbers represent % cells in the gate. One-way ANOVA with Tukey's posttest. (*C*) Nur77 expression in EADN cells of wild-type or MHC knockout (I-Ab-/-.b2m-/-), non-TCR transgenic mice, shown as median fluorescence intensity (mFI) from intracellular staining and flow cytometry. Unpaired, two-tailed Student's *t* test. (*D*) OT-1.$RAG2^{-/-}$.$\beta2M^{-/-}$ fetal thymic lobes were cultured in the presence or absence of antigenic peptides with exogenously added β2M for 24 h. CD69 up-regulation is shown for stringently gated $CD4^-CD8^-$ DN cells. Each point represents an individual thymic lobe. (*E*) SPADE of B6 $Thy1^+$ DN thymocytes. Thymocytes are pregated as $Thy1.2^+CD4^-CD8\alpha^-$ before performing SPADE using 12 other surface markers (*Materials and Methods*). $^{**}P < 0.01$ $^{***}P < 0.001$.

EADN as Earliest Identifiable Developmental Stage in a Human T-ALL Case. From five clinical T-ALL cases seen at University Hospital-Missouri (2016 to 2018), we found evidence of EADN as the earliest identifiable developmental stage in one case. The neoplastic population in peripheral blood included a hallmark heterogeneous $CD4^+$ $CD8^+$ DP subset and a DN subset (Fig. 3*A*, *Top*). Comparing T-lineage ($CD7^+$) cells in various subsets, CD8SP cells were $CD3^+$ (Fig. 3*B*, *Top Left*), while the heterogeneous DP tumor population showed down-regulated surface CD3 (Fig. 3*B*, *Top Middle*), a trait in common with nontransformed thymic DP cells (29). All DN cells that were T-lineage ($CD7^+$) were surface $CD3^+$ (Fig. 3*B*, *Top Right*), unlike nontransformed thymic DN counterparts, and $CD45^{dim}$ (Fig. 3*C*, *Top* and *SI Appendix*, Fig. S3), indicating that they were immature and neoplastic. Additionally, immunohistochemistry (IHC) staining of bone marrow demonstrated infiltration of neoplastic cells expressing TCRβ but not γδTCR (Fig. 3*D*, *Top*). This indicates that transformation occurred at a developmental stage postcommitment to αβ-lineage. Collectively, this case provided evidence that transformation may have occurred at the EADN cell stage.

A contrasting example is a second case in which transformation apparently occurred at an earlier developmental stage than EADN. Peripheral blood showed similar T cell subsets (Fig. 3*A*, *Bottom*) with CD8SP surface $CD3^+$ (Fig. 3*B*, *Bottom Left*). But DP cells did not down-regulate surface CD3 (Fig. 3*B*, *Bottom Middle*), and DN neoplastic cells were $CD7^+$ but surface CD3 negative-to-low (Fig. 3*B*, *Bottom Right*). Gating on the few $CD7^+$ DN cells that were highest for surface CD3, their CD45 level was similar to that observed for CD8SP cells, indicating these were mature, peripheral DN T cells, while the $CD7^+$ DN CD3 negative-to-low cells were $CD45^{dim}$, indicating immaturity and transformation (Fig. 3*C*, *Bottom*). IHC staining revealed tumor cells expressing either TCRβ or γδTCR,

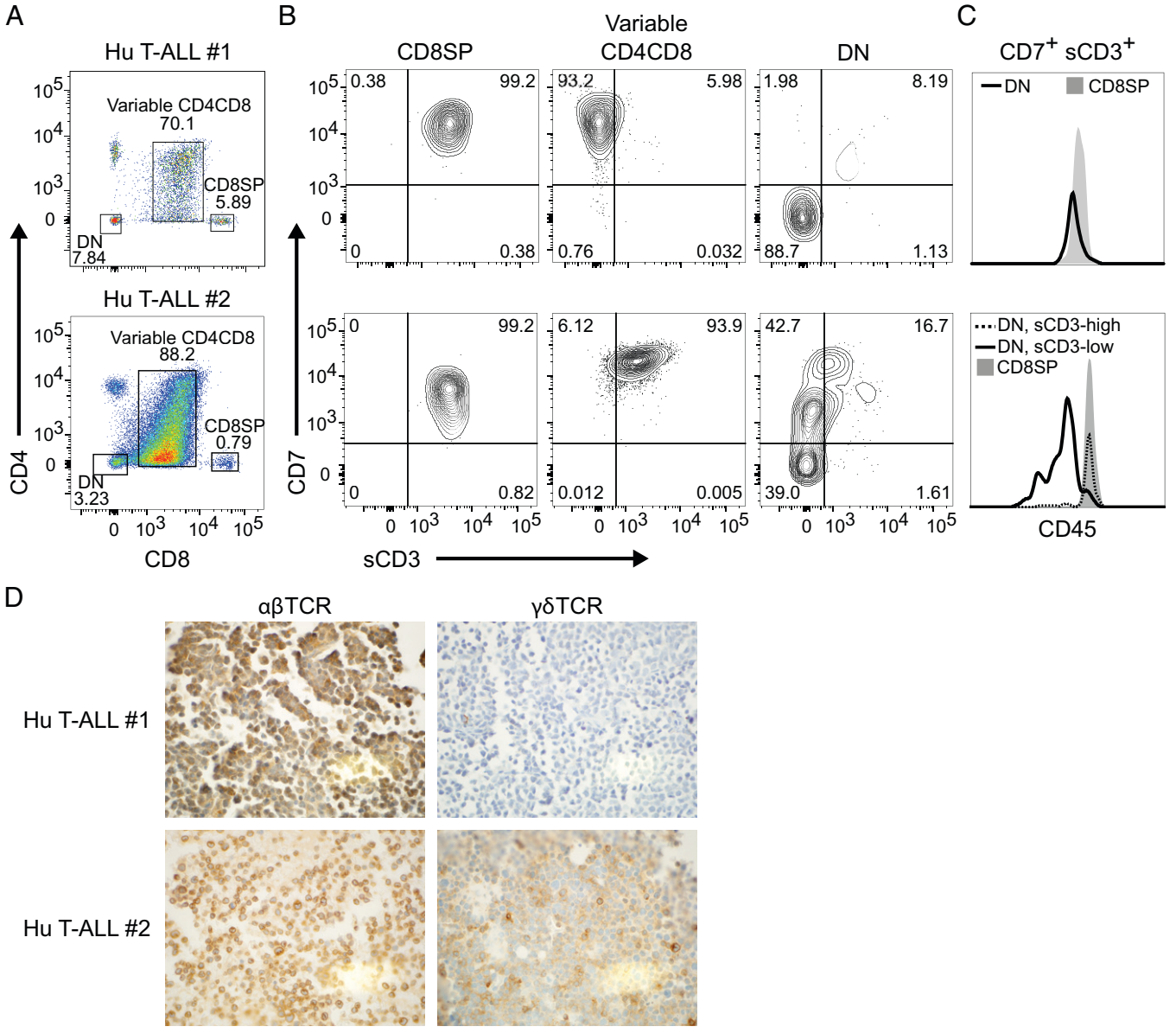

Fig. 3. EADN represents phenotypically earliest stage in a human T-ALL case. (*A*) Surface CD4/CD8 profiles of peripheral blood T cells from 2 T-ALL patients. (*B*) CD8SP, variable CD4/CD8 expressing, and DN cells are further analyzed for surface CD3 expression. CD7 is used as a T-lineage marker. Quadrants are set using isotype controls. (*C*) Expression of CD45 on neoplastic and healthy T cells in the $CD7^+CD3^+$ gated cells from (*B*). Numbers in flow cytometry plots represent % cells in respective gates. (*D*) Immunohistochemistry staining for αβTCR (*Left*) and γδTCR (*Right*) of patient cells (bone marrow, original magnification ×600).

indicating transformation at a developmental stage preceding commitment to αβ lineage (Fig. 3*D*, *Bottom*). We conclude that in this second case transformation likely occurred in a cell at an earlier developmental stage than EADN, thus retaining both αβ and γδ T-lineage potential.

Spontaneous EADN T-ALL Transformation in OT-1 Mice. We observed that OT-1 mice spontaneously developed T cell leukemic lymphomas with features resembling human T-ALL with EADN as earliest identifiable stage. Leukemic OT-1 mice appeared moribund and presented with enlarged spleen, thymus, and lymph nodes (Fig. 4*A*). Flow cytometry analysis revealed that hypertrophic lymphoid organs were infiltrated by $Thy1^+$ T-lineage blasts (Fig. 4 *B* and *C*), which expressed OT-1 TCR (Fig. 4*D*) along with heterogeneous coreceptor expression, ranging from DN to immature CD8 single-positive (iSP) to DP. Three primary tumor examples are shown (spleen, Fig. 4 *E*–*H*; thymus and gut lymph nodes, *SI Appendix*, Fig. S4*A*; T-ALL OT-1 tumors abbreviated Tot). In vivo passaging was performed by intravenous retro-orbital injection into nonirradiated C57BL6/J (B6) recipients. By 3 to 4 wk, all recipients became moribund reaching euthanasia criteria as tumors infiltrated lymphoid organs (*SI Appendix*, Fig. S4*B*). Although in vitro cell passaging was attempted and failed in early generations, serial passaging in vivo led to increased tumor growth rate, shorter time to reaching endpoint criteria, and eventual acquisition of a tumor cell line that readily passages in vitro (Tot-1si). Due to the immature T-lineage of these tumors, acute growth rate upon transplantation, blasted cell size and granularity, and leukemic dissemination, we conclude that their classification is T-ALL.

We investigated if the NOTCH signaling pathway was dysregulated in these tumors, as predicted for T-ALL (6). *NOTCH1* sequencing revealed frameshift mutations in all primary tumors assessed, resulting in loss of the regulatory PEST domain (*SI Appendix*, Table S1). Importantly, each tumor's mutation was unique and heterozygous, establishing the clonal origin of each tumor. At the NOTCH1 protein level, we compared B6 wild-type thymocytes (nontransformed) with high-leukemia-load organs from different Tot-bearing mice, finding in the tumor samples induced expression of both full-length and cleaved NOTCH1 products (Fig. 4*I*). Antibody specificity for NOTCH1 was validated by the inclusion of thymus cells from a mouse with conditional deletion of CBP, known to increase NOTCH1 activation (30). The Tot-1si cell line expressed a vast excess of cleaved NOTCH1 and failed to grow when cultured in the presence of γ-secretase inhibitor, Compound E (Fig. 4*J*), indicating that NOTCH1 signaling was required for tumor maintenance.

Because EADN stage was the earliest developmental stage observed in OT-1 T-ALL, we hypothesized that EADN stage might be specifically susceptible to transformation. However, an alternative hypothesis was that tumor originated from post-positive selection cells at late DP or SP stages, the stages in normal T cell development where surface TCR is up-regulated toward full expression level (29). To distinguish between these hypotheses, we performed gene expression microarray analysis of Tot-1si tumor followed by unsupervised hierarchical clustering with normal thymocytes of various developmental stages from protocol-matched ImmGen data (31). Transcriptionally, Tot-1si cells most closely resembled immature subsets surrounding β-selection (DN3a, DN3b, DN4, iSP; Fig. 5), and was relatively dissimilar to the most immature subsets (ETP, DN2) and the more mature subsets (DP, SP) and other subsets (NKT, GDT; Fig. 5; statistical significance of HC branch points

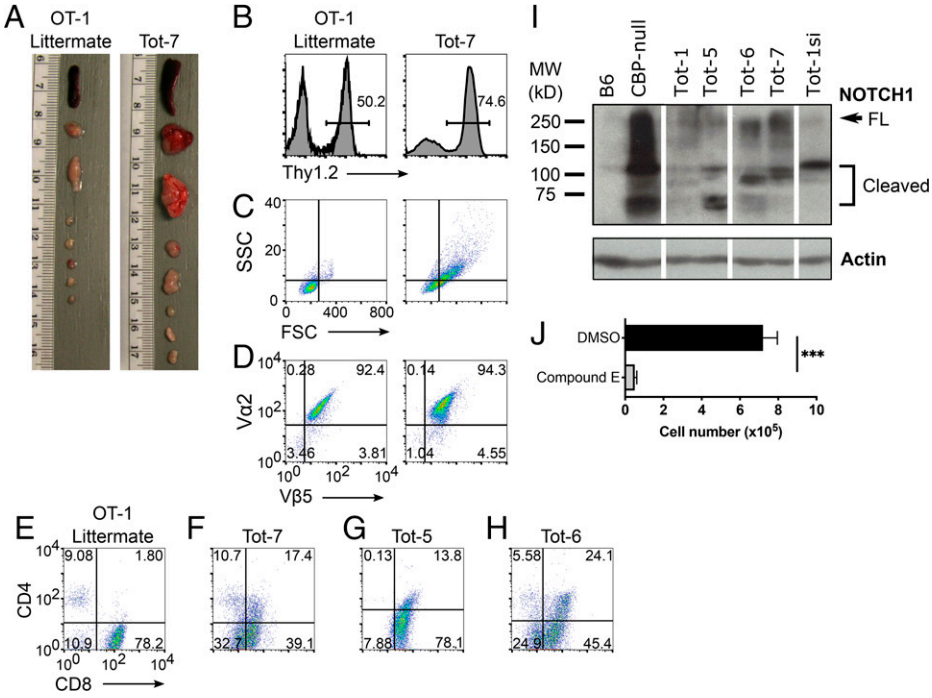

Fig. 4. Spontaneous EADN T-ALL transformation in OT-1 mice. (*A*) Lymphoid organs in leukemic mice are enlarged compared to healthy littermates. *Top* to *Bottom*: spleen, thymus, gut lymph nodes, various peripheral lymph nodes. (*B*) Frequency of T-lineage cells ($Thy1.2^+$) in healthy OT-1 littermate (*Left*) and primary leukemic (*Right*) spleens. (*C*) Flow cytometry analysis comparing the size (FSC) and granularity (SSC), (*D*) OT-1 TCR surface expression, and (*E*) CD4/CD8 expression of healthy OT-1 and (*F*–*H*) primary OT-1 T-ALLs assessed in splenocytes. Numbers in flow cytometry plots represent frequency of cells in respective gates. (*I*) Western blot of lysates prepared from wild-type B6 thymocytes, CBP-null thymocytes, OT-1 T-ALL tumors as named, and an OT-1 T-ALL tumor cell line grown in vitro (Tot-1si). Lysates were immunoblotted for NOTCH1 expression. Actin was assessed as a loading control, where B6 thymocytes were intentionally overloaded to amplify NOTCH1 detection from that sample. (*J*) Tot-1si cells (2.5×10^5) were seeded and cultured in the presence of DMSO vehicle control or the gamma-secretase inhibitor, Compound E. Unpaired, two-tailed Student's *t* test, $^{***}P < 0.001$.

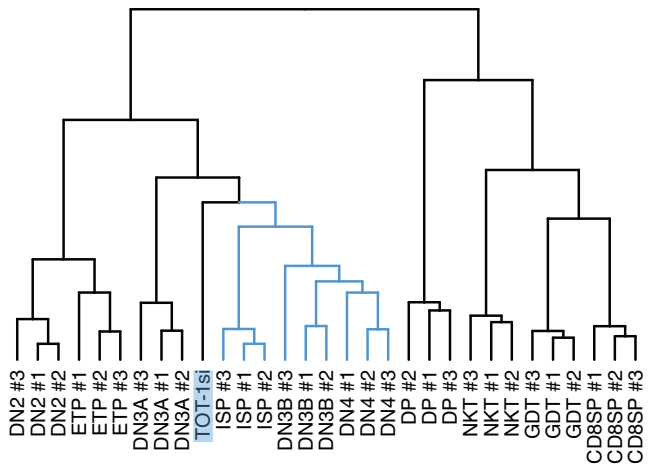

Fig. 5. OT-1 T-ALL transformation occurs at the immature, EADN stage. Hierarchical clustering of gene expression data of Tot-1si leukemic cells (label highlighted in blue) and wild-type progenitor and mature T cell subsets (31). Branches of subsets that bear the closest similarity to the tumor represent immediate-post-β-selection stages, and their branches are colored blue. DN, $CD4^{-}CD8^{-}$ double negative. ETP, early thymic progenitor. ISP, immature single positive. DP, $CD4^{+}CD8^{+}$ double positive. NKT, natural killer T cell. GDT, γδ T cell. SP, single positive.

shown in *SI Appendix*, Fig. S5*A*). This result led to a prediction that an initiating tumor cell that was post-β-selection, but prepositive-selection might generate progeny with many different TCRα gene products from endogenous loci. The reasoning was that tumor proliferation would occur before the DP positive selection step that halts TCRα rearrangement (32). Mouse TCRα spectratyping was performed, revealing that while all Tot tumors expressed the transgenic TCRα (Vα2), Tot-1, -5, and -7 expressed numerous other TCRα gene products, indicating that diverse TCRα rearrangement could continue posttransformation (*SI Appendix*, Fig. S5*B*). These gene expression patterns favor the hypothesis that EADN cells close to the β-selection checkpoint may be specifically susceptible to T-ALL oncogenesis in the OT-1 system.

MHC is Required for EADN-Stage OT-1 T-ALL Initial Oncogenesis But Not Late Growth. To investigate the role of αβTCR signaling in the generation of OT-1 T-ALL, we followed the frequency of T-ALL in mice in the presence or absence of OT-1 TCR and MHC class I in a cohort study (Table 1). We observed that the incidence of T-ALL in OT-1 mice was ∼10% in the 3- to 9-mo age group, with no incidence in wild-type B6 mice aged in parallel, the latter expected from published low-incidence rates (33). In contrast, T-ALL failed to develop in OT-1.$\beta2M^{-/-}$ mice, which lack MHC class I necessary for positive selection signaling through OT-1 TCR (34). When MHC class I was reintroduced by breeding OT-1.$\beta2M^{-/-}$ mice to wild-type B6 mice, T-ALL was observed among $OT\text{-}1^{+}$ F1 progeny. RAG-mediated DNA rearrangement was not required for transformation since OT-1.$AG2^{-/-}$ mice were observed to develop T-ALL. Finally, we also observed OT-1 T-ALL oncogenesis in F1 progeny from OT-1 x B6Ly5.1 mice from a separate investigator's colony housed at a different institution (Table 1). These results suggest that MHC is required for Tot tumor leukemogenesis.

Table 1. Population study demonstrating a requirement for MHC class I for spontaneous T-ALL development in OT-1 mice

Genotype	T-ALL incidence	Age
WT (B6)	0% (0/30)	3–9 mo
OT-1	10% (5/50)	3–9 mo
OT-1.$\beta2M^{-/-}$	0% (0/190)	3–12 mo
OT-1.$Rag2^{-/-}$	+	
OT-1.$\beta2M^{-/-}$ x B6 (F1)	+	
OT-1 x B6 Ly5.1 (F1)	+	

(*Top*) Percent incidence is listed along with mouse numbers (incidence/total). (*Bottom*) Observation of OT-1 T-ALL tumors in other genotypes without controlled population study are listed with "+".

To determine if the requirement for MHC class I could be lost upon extended tumor growth beyond initial oncogenesis, Tot tumors were transplanted into wild-type B6 or $\beta2M^{-/-}$ recipients. As described above, tumor growth occurred in wild-type B6 mice, but tumors initially failed to grow when recipient MHC class I was absent (example, early passage Tot-1, *SI Appendix*, Fig. S6 *A*, *B*, and *E*). However, the same tumor line after multigeneration passaging and now tested in parallel, Tot-1si, acquired the ability to grow in $\beta2M^{-/-}$ recipients (*SI Appendix*, Fig. S6 *C–E*), and also grew in MHC class I and II double-knockout recipients (*SI Appendix*, Fig. S6 *F–H*). Tot-1si grew independently in vitro, with surface phenotype matching that of EADN cells, at DN3b with full surface TCR expression (Fig. 6*A*). Although this multipassage T-ALL did not require MHC for growth, it responded to antigen-presenting cells (APCs) with peptides loaded in H-2Kb. Tot-1si cells exhibited graded up-regulation of CD69 in response to weak Q4H7 peptide and strong OVA peptide above the null-peptide, FARL (Fig. 6*B*). These responses were equivalent in the presence or absence of anti-CD8 blocking mAb (Fig. 6*B*), although the blocking mAb inhibited responses to the stimulatory peptides from mature CD8SP OT-1 T cells (*SI Appendix*, Fig. S6*I*). These data support a model in which the naturally low-frequency EADN subset, magnified to high representation in the OT-1 system, is capable of coreceptor-independent TCR:MHC signaling that provides a causal pathway for T-ALL oncogenesis susceptibility (*SI Appendix*, Fig. S7).

Discussion

Signals that drive T cell development can also play a role in T-ALL cancer development (35). In T-ALL, thymocytes arrest at different developmental stages defined by both immunophenotype and transcription profile, reflecting the cellular context at which transformation has occurred (36). Furthermore, T-ALL can present with neoplastic cells at different developmental stages among patients, and within tumor cell populations in single patients, where various developmental, signaling, and/or mutational pathways of leukemogenesis are possible (1, 36). Hyperactive NOTCH is a central, signature feature that cooperates with both upstream and downstream signals and mutations for leukemic transformation (6, 37, 38). Among the best characterized NOTCH-synergizing partners in T-ALL initialization are the earliest known forms of immature TCR/CD3 signaling that do not require MHC-dependent ligation (7–9).

By contrast, in this study we showed MHC-dependent development of T-ALL bearing mutations in NOTCH1, involving the understudied condition where thymocytes display early αβTCR at DN (EADN) stage. In normal T cell development, we validated that EADN cells exist as once reported (14), and their low frequency can be similar in mouse and human (Fig. 1). Apart from their full-level αβTCR surface expression, EADN cells showed DN3b-DN4 staging expressing markers of immature progenitor cells and required CD3δ but not MHC for their generation/detection (Figs. 1 and 2). When a case of human T-ALL showed

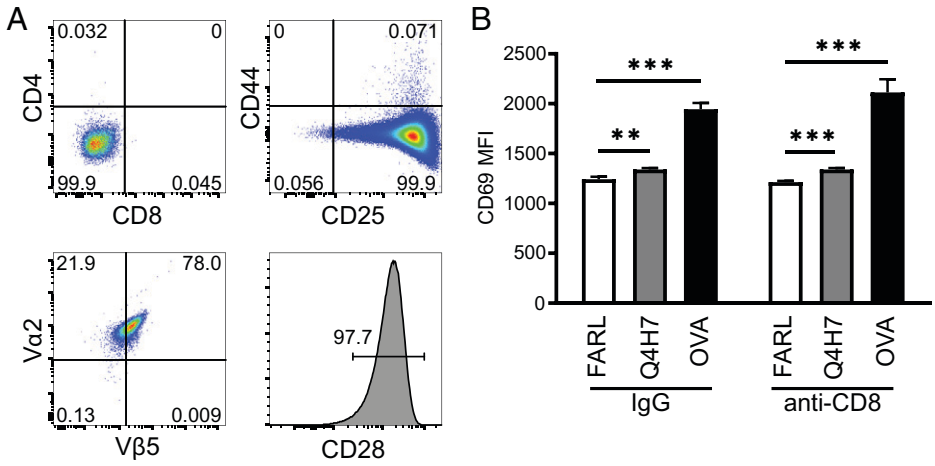

Fig. 6. EADN-stage OT-1 T-ALL cells are capable of coreceptor independent MHC engagement. (*A*) Tot-1si was derived from the most immature-appearing tumor cells adapted to culture after serial transplantation in B6 recipients. Tot-1si was analyzed for surface CD4/CD8 and OT-1 TCR expression. Tot-1si DN subset categorization was determined by CD44/CD25 expression, and post-β-selection status was determined by CD28 expression level. (*B*) Surface level of CD69 induced in Tot-1si cells incubated with null (FARL), weak (Q4H7), or strong (OVA) antigenic peptides presented by APCs. Cells were cultured overnight with 2 μM peptide and APCs, with anti-CD8 blocking antibody or irrelevant IgG control. Numbers in flow cytometry plots represent frequency of cells in respective gates. Error bars represent SEM. Unpaired, two-tailed Student's *t* test, $*P < 0.05$ $***P < 0.001$.

EADN cells as the earliest identifiable developmental stage, a TCR transgenic mouse system was sought that could model the EADN condition and was found in OT-1 where susceptibility to EADN T-ALL oncogenesis was also observed (Figs. 3–5).

Primary EADN cells and OT-1 EADN T-ALLs responded to MHC-based ligands in a coreceptor-independent manner. First, MHC expression in vivo increased Nur77 in polyclonal EADN cells in the absence of TCR transgenes (Fig. 2*C*). Next, OT-1 EADN cells up-regulated CD69 in response to strong agonist OVA peptide provided in fetal thymic organ culture (FTOC) (Fig. 2*D*), while Tot-1si cells up-regulated CD69 when weak (Q4H7) or strong (OVA) peptides were presented in vitro (Fig. 6*B*). Because these responses were not expected since OT-1 is generally a CD8-dependent TCR (26), coreceptor independence was confirmed when anti-CD8 blocking mAb had no effect against the Tot-1si responses, but inhibited CD69 up-regulation from peripheral OT-1 T cells (*SI Appendix*, Fig. S6*E*). This suggests that even though EADN cells lack coreceptor, they possess an intrinsically high sensitivity to MHC-based ligands that must become down-regulated upon further cell maturation. Such developmental tuning of antigen recognition is known to apply to DP-SP transition based on regulation of CD8 sialylation and other processes (39, 40), and may extend earlier when there is EADN expression to DN-DP-SP, representing highest-to-lowest αβTCR sensitivity (41) and least-to-most coreceptor dependence.

Interestingly, MHC class I was required for OT-1 mice to produce T-ALLs that showed EADN as the earliest identifiable developmental stage among mostly DP-heterogenous tumor populations (Fig. 6), a phenotype shared with the human T-ALL case #1 (Fig. 3). Compared with 10% T-ALL incidence in OT-1, the OT-1.β2M$^{-/-}$ genotype produced no tumors, and we extended the age range and mouse number but still found 0/190 (Table 1). Numerous other mouse experimental systems have observed T-ALL oncogenesis previously, but not this requirement for MHC (42, 43). We further emphasize that, in our model, the genetic background is one of positive selection of OT-1, such that only weak αβTCR:MHC signals are expected in vivo (34). We hypothesize that the MHC-requirement may be specific for EADN-stage T-ALL initiation, whereas tumorigenesis initiated at earlier stages is MHC-independent; but common to both pathways, bulk tumor populations can share heterogeneous DN-DP phenotype as they continue to follow the T cell developmental program (*SI Appendix*, Fig. S7). First, mRNA expression of all CD3 subunits is present from DN1 and sustained through all subsequent stages (44), although CD3 function in normal T cell development is not required until pre-T cell signaling at DN3 (45). Clonotype-independent CD3 complexes may synergize with NOTCH mutation to drive T-ALL and increase this activity when engaged by injectable anti-CD3 mAb (9) or when joined by unnaturally early, prerearranged αβTCR (42, 46). Next, pre-Tα expression begins by DN3a to join TCRβ forming pre-TCR, with β-selection advancing cells to DN3b, DN4, iSP, and DP (44). Pre-TCR signals are thought to drive many models of T-ALL (7, 8) without a role for MHC, although some evidence suggests pre-TCR can play a facilitating rather than requisite role, perhaps depending on the dose of NOTCH signaling (9). Expression of other transgenic TCRs often occurs at unnaturally early DN1 or DN2 stages, which subsequently at DN3 stage provides signals equivalent to pre-TCR to advance development (14, 47, 48) and perhaps plays a ligand-independent role in T-ALL tumorigenesis. Further, a TCR transgenic mouse with strong reactivity against a self-antigen (survivin) that would model thymic negative selection was found to have full αβTCR expression at DN1. DN T-ALLs developed in these mice in the presence or absence of MHC class I, although MHC-sufficient animals succumbed at a faster rate (49). Finally, αβTCR has been previously implicated in retrovirus-induced leukemogenesis by serving as a direct retrovirus receptor for thymocyte infection (50–53) and providing mitogenic signals to promote proliferation of cells expressing oncogenes (54–56). The present data provide evidence for an MHC requirement for T-ALL initiation, a property that may be specific for the unique EADN developmental condition, where the timing of full-level αβTCR surface expression at DN3 is modeled in the OT-1 system. Furthermore, here, thymic positive selection is driven by weak self-peptide-MHC ligands, without strong reactivity and negative selection, and this characteristic may also influence the MHC-dependent induction of T-ALL observed.

Although MHC was required to initiate tumorigenesis, propagation in vivo saw the MHC requirement lost (*SI Appendix*, Fig. S6 *A* and *B*), while tumor aggression increased and an MHC-independent cell line was established that could grow, in vitro (*SI Appendix*, Fig. S6 *C* and *D*). In general, cancer

progression can involve loss of dependence on some receptors or pathways while mutation accumulation and selection allow other pathways to replace survival and proliferation signals (35, 36). Some T-ALL models that begin with heavy reliance on pre-TCR signals may lose that receptor addiction during tumor maintenance (9). In our OT-1 T-ALL model, it is curious that passaging in vivo in the presence of MHC ligand might create selection pressure that favors outgrowth of tumors that lose MHC-dependence. One might speculate that with both donor tumors and recipient mice expressing syngeneic MHC class I during passaging (*SI Appendix*, Fig. S6*B*), MHC may not be limiting unless specificity of peptide presentation also matters. If so, it might be interesting to identify self-peptide-MHC complexes that stimulate T-ALL oncogenesis and early growth.

The present study implicates signaling through MHC:αβTCR as a required driver event in NOTCH-dependent T-ALL oncogenesis when initiating cells are EADN in the presence of positive selection-strength MHC. The data illustrate how unique developmental states provide unique context and signaling rules that govern precursor T cell reactivity and T-ALL leukemogenesis. It is likely that a deeper understanding of both overlapping and disparate mechanisms driving T-ALL between different models and thymocyte stages will create more knowledge surrounding the heterogeneity of T-ALL clinical phenotypes. The identification of EADN as a distinct developmental state at risk for transformation may inform future stratification of therapy regimens for T-ALL.

Materials and Methods

Mice. All mice were C57BL6 background. OT-1 mice were originally provided by Larry R. Pease (Mayo Clinic), and were further bred to β2M$^{-/-}$ (Jackson Laboratory) to obtain OT-1.β2M$^{-/-}$ mice. β2M$^{-/-}$ mice were bred to MHC II$^{-/-}$ (57) to obtain MHC I$^{-/-}$.MHC II$^{-/-}$ double knockout mice. CD3ε$^{-/-}$ζ$^{-/-}$ mice were originally provided by D. Vignali (then at St. Jude Children's Research Hospital) with permission from C. Terhorst (Beth Israel Deaconess Medical Center, Harvard Medical School). CD3δ$^{-/-}$ mice were a kind gift from Dietmar Kappes (Fox Chase Cancer Center, Philadelphia, PA), subsequently bred to MHC I$^{-/-}$.MHC II$^{-/-}$ mice to obtain CD3δ$^{-/-}$.MHC I$^{-/-}$.MHC II$^{-/-}$ mice. OT-1.RAG2$^{-/-}$ mice were originally purchased from Taconic Biosciences. Mice were bred and/or maintained at University of Missouri-Columbia or the Mayo Clinic, and all animals were housed in specific pathogen-free facilities. Within experiments, mice were age- and sex-matched between experimental groups. Individual mice within 15 d of age were accepted as age matched. All mouse care and experimentation adhered to institutional guidelines and the NIH Guide for the Care and Use of Laboratory Animals.

Cell Culture. Tot-1si cells were maintained in RPMI-1640 (Life Technologies) supplemented with 10% Cosmic calf serum (HyClone), 2 mM L-glutamine (Life Technologies), 1% nonessential amino acids (Gibco), 1 mM sodium pyruvate, penicillin (100 U/mL)/streptomycin (100 μg/mL) (Life Technologies), and sometimes 0.02% Fungizone (Gibco), and were cultured in a 37 °C incubator with 5% CO_2.

In Vitro T Cell Stimulation. Tot-1si cells (2.5×10^5) or mature T cells from OT-1.RAG2$^{-/-}$ splenocytes (0.4×10^6) were resuspended in 200 μL complete RPMI media in a 96-well plate. To assess coreceptor-independent TCR activation, cells were preincubated with 10 μg/mL anti-CD8α blocking antibody (clone 53-6.7, BioLegend) or nonimmune rat IgG (BioLegend) for 30 min at 37 °C. Next, Tot-1si cells were mixed with an equal number of CD3ε$^{-/-}$ζ$^{-/-}$ splenocytes as APCs and resuspended in 200 μL complete RPMI media in a 96-well plate. To the coculture, and to the OT-1.RAG2$^{-/-}$ splenocytes in parallel, peptide antigens FARL, Q4H7, or OVA were added at a final concentration of 2 μM and incubated overnight at 37 °C. Cells were harvested and subjected to flow cytometry analysis.

FTOC. Timed matings were performed, as previously described (58). Briefly, mouse cages were divided in half using an acrylic divider. One male and one female mouse resided on each side of a divided cage for ~72 h, after which the divider was removed in late afternoon to allow mating overnight. FTOC was performed as previously described (34). Fetal thymi were harvested on embryonic day 15. Each fetal thymic lobe was placed on sterile mixed cellulose ester gridded filter paper (Millipore) on top of a Gelfoam sterile sponge (Pfizer), in HyClone CCM1 serum-free media (GE Life Sciences) in one well of a 48-well plate. Some cultures were supplemented with exogenous human β2M (5 μg/mL, Sigma) and peptides FARL (SSIEFARL), Q4H7 (SIIQFEHL), or OVA (SIINFEKL) at the indicated concentrations. Thymi were cultured for 24 h at 37 °C before harvest and analysis by flow cytometry.

Flow Cytometry. Whole thymocyte or peripheral organ single-cell suspensions were prepared as previously described (34). FcR binding was blocked with anti-mouse CD16/32 antibody (BioLegend) at room temperature for 15 min before staining. Sample acquisition was performed using either BD LSRFortessa X-20, Accuri C6, or BD FACSCalibur instruments. Data analyses were done using FlowJo v10. For anti-mouse antibodies, CD4 (GK1.5), CD5 (53-7.3), CD8α (53.6-7), CD8β (53-5.8), CD25 (3C7), CD28 (37.51), CD44 (IM7), CD45.2 (104), CD69 (H1.2F3), CD90.2 (30-H12), CD117 (ACK2), CD122 (TM-β1), γδTCR (GL3), H-2K^b (AF6-88.5), NK1.1 (PK136), PD-1 (29F.1A12), TCRβ (H57-597), Vα2 (B20.1), Vα3.2 (RR3-16), Vα8.3 (B21.14) were purchased from BioLegend. Anti-Nur77 (12.14) was purchased from ThermoFisher Scientific. The tetramer CD1d-PBS57 was obtained from the NIH Tetramer core facility. For anti-human antibodies, CD1a (HI149), CD3 (SK7), CD4 (SK3), CD5 (L17F12), CD7 (CD7-6B7), CD8α (SK1), CD28 (CD28.2), CD34 (581), CD45 (2D1), CD56 (5.1H11), αβTCR (IP26), γδTCR (B1) were purchased from BioLegend. CD7 (M-T701) and CD56 (NCAM16.2) were purchased from BD Biosciences. In certain samples viability dyes were used: TOPRO3 (ThermoFisher Scientific), 7-AAD (BD Biosciences).

SPADE Analysis. SPADE analysis was performed using Cytobank (59) using a target setting of 75 nodes at 10% downsampling. After gating on Thy1.2+CD4$^-$CD8$^-$ DN cells, DN cells were clustered using TCRβ, CD1d-tetramer (PBS57), γδTCR, NK1.1, H2K^b, PD-1, CD5, CD25, CD28, CD44, CD122, and pooled TCRVαs (Vα2, Vα3.2, and Vα8.3). Cell population assignment was done using established markers for lineage and developmental maturity. Surface expression data that is displayed in heatmaps represent log-like transformed median fluorescence intensity, following standard Cytobank analysis protocols.

Intracellular Nur77 Staining. Single cell suspensions of thymocytes were fixed and permeabilized using Cytofix/Cytoperm kit (BD Biosciences) according to manufacturer instructions and stained with PE-anti-Nur77 antibody (clone 12.14, eBioscience) or mouse IgG1 isotype control (clone P3.6.2.8.1, eBioscience) for 30 min, on ice. As positive control for Nur77 staining, OT-1.RAG2$^{-/-}$ splenocytes (0.4×10^6 cells/well) were stimulated with 2 μM OVA peptide for 2 h at 37 °C.

NOTCH1 Expression and Mutation Analysis. OT-1 T-ALL tumors, control thymocytes, and the CBP-null thymocytes were lysed in Nonidet P-40 lysis buffer (1% Nonidet P-40, 0.5% sodium deoxycholate, 5 mM EDTA, 50 mM Tris pH 7.4, 150 mM NaCl, and protease inhibitors). Lysates were centrifuged at 14,000 rpm for 15 min at 4 °C. Protein samples were separated by SDS-PAGE, transferred to nitrocellulose membrane and detected by Western blot analysis using standard techniques. Blots were probed with antibodies that recognize NOTCH1 (mN1A, Santa Cruz Biotechnology) and Actin (Millipore). Genomic DNA was amplified by PCR and sequenced using 2 sets of primers (60) for exon 34 of NOTCH1. Forward (1): 5′-GCTCCCTCATGTACCTCCTG-3′. Reverse (1): 5′-TAGTGGCCCCATCATG CTAT-3′. Forward (2): 5′-ATAGCATGATGGGGCCACTA-3′. Reverse (2): 5′-CTTCACCCT GACCAGGAAAA-3′.

Microarray Analysis. Total RNA from Tot-1si cells was extracted using Qiagen RNeasy Mini kits (Qiagen). RNA quality assessment was done using an Agilent 2100 Bioanalyzer, followed by hybridization to Affymetrix MoGene 1.0 ST array. Data for normal thymocyte subsets were retrieved from the ImmGen microarray dataset GSE15907 (31). Raw feature data were $\log_2$ transformed, background corrected, and normalized using the robust multi-array average (RMA) method with the 'oligo' package (61). Low intensity probes were filtered out, resulting in 2,619 probes being included in the unsupervised hierarchical clustering. Hierarchical clustering was performed using Ward's method. Dissimilarities between clusters were calculated using Euclidean distance. To assess the uncertainty of the hierarchical clustering, approximately unbiased (AU) value (62) was used as the uncertainty metric. AU values were calculated using the package 'pvclust'

(63) with 10,000 bootstrap replications. All procedures were performed using R (version 4.0.5). Data used in this study have been deposited in the NCBI Gene Expression Omnibus under the GEO series accession number GSE180556.

TCRα Spectratyping. TCRα spectratype analysis was performed with primer sequences and protocols as previously described in detail (64).

Patient Samples and Data. University of Missouri Institutional Review Board (IRB) guidelines and protocols were followed for retrospective analysis of clinical patient T-ALL data (IRB approval number 2011050). Pediatric thymic tissue was provided from de-identified medical waste by an approved organ procurement organization, with a full waiver of consent approved by IRB approval number 2011876.

IHC. Formalin-fixed paraffin-embedded bone marrow sections were manually stained according to standard procedures. Mouse anti-human TCRδ antibody (clone H41, Santa Cruz Biotechnology) and mouse anti-human TCRβ (βF1, clone 8A3, ThermoFisher Scientific) were used to detect human γδTCR and αβTCR, respectively. The sections were then immunoperoxidase stained with hematoxylin counterstaining. Positive and negative controls were included for each stain.

Statistical Analysis. Prism (version 8, GraphPad Software) and R were used for statistical analysis. Unless otherwise indicated, for comparison of two groups, unpaired Student's *t* test was used; for comparison of multiple groups, one-way ANOVA with Tukey's posttest was used. All error bars represent SEM.

Data Availability. Microarray data have been deposited in National Center for Biotechnology Information, Gene Expression Omnibus Accession no. GSE180556 and can be accessed at https://www.ncbi.nlm.nih.gov/geo/query/acc.cgi?acc=GSE180556. (65)

ACKNOWLEDGMENTS. For technical help and scientific advice, we thank Donald Doll, MD, in Hematology & Medical Oncology at University Hospital, Missouri, the Cell & Immunobiology Core at University of Missouri-Columbia, and Flow Cytometry and Genome Analysis Cores at Mayo Clinic Rochester. We thank the NIH tetramer core facility at Emory University for providing SIIINFEKL/H-2Kb and PBS-57/CD1d tetramers. This project was supported by an AAI Intersect Fellowship (to K.G.L., A.G.S.), Pilot Project Award from consortium partnership Ellis Fischel Cancer Center (EFCC) and Siteman Comprehensive Cancer Center (SCCC) (to A.G.S), institutional funds of University of Missouri-Columbia (to A.G.S., D.G.) and Mayo Clinic (to A.G.S., D.G.), and NIH Grant R01GM103841 (to A.G.S.).

Author affiliations: [a]Department of Molecular Microbiology & Immunology, School of Medicine, University of Missouri-Columbia, Columbia, MO 65212; [b]Department of Immunology, Mayo Clinic College of Medicine, Rochester, MN 55095; [c]Department of Pediatrics, Mayo Clinic College of Medicine, Rochester, MN 55095; [d]Department of Surgery, Mayo Clinic College of Medicine, Rochester, MN 55095; [e]Department of Surgery, School of Medicine, University of Missouri-Columbia, Columbia, MO 65212; [f]Clinical Flow Cytometry Laboratory, University Hospital, University of Missouri-Columbia, Columbia, MO 65212; [g]Department of Pathology & Anatomical Sciences, School of Medicine, University of Missouri-Columbia, Columbia, MO 65212; and [h]Department of Biomedical, Biological, & Chemical Engineering, College of Engineering, University of Missouri-Columbia, Columbia, MO 65212

1. L. Belver, A. Ferrando, The genetics and mechanisms of T cell acute lymphoblastic leukaemia. *Nat. Rev. Cancer* **16**, 494–507 (2016).
2. C. H. Pui, W. E. Evans, Acute lymphoblastic leukemia. *N. Engl. J. Med.* **339**, 605–615 (1998).
3. C. H. Pui *et al.*, Childhood acute lymphoblastic leukemia: Progress through collaboration. *J. Clin. Oncol.* **33**, 2938–2948 (2015).
4. S. S. Winter *et al.*, Improved survival for children and young adults with T-lineage acute lymphoblastic leukemia: Results from the children's oncology group AALL0434 methotrexate randomization. *J. Clin. Oncol.* **36**, 2926–2934 (2018).
5. V. Asnafi *et al.*, Analysis of TCR, pT alpha, and RAG-1 in T-acute lymphoblastic leukemias improves understanding of early human T-lymphoid lineage commitment. *Blood* **101**, 2693–2703 (2003).
6. A. P. Weng *et al.*, Activating mutations of NOTCH1 in human T cell acute lymphoblastic leukemia. *Science* **306**, 269–271 (2004).
7. D. Allman *et al.*, Separation of Notch1 promoted lineage commitment and expansion/transformation in developing T cells. *J. Exp. Med.* **194**, 99–106 (2001).
8. D. Bellavia *et al.*, Combined expression of pTalpha and Notch3 in T cell leukemia identifies the requirement of preTCR for leukemogenesis. *Proc. Natl. Acad. Sci. U.S.A.* **99**, 3788–3793 (2002).
9. A. F. Campese *et al.*, Notch1-dependent lymphomagenesis is assisted by but does not essentially require pre-TCR signaling. *Blood* **108**, 305–310 (2006).
10. I. Maillard *et al.*, The requirement for Notch signaling at the beta-selection checkpoint in vivo is absolute and independent of the pre-T cell receptor. *J. Exp. Med.* **203**, 2239–2245 (2006).
11. D. K. Shah, J. C. Zúñiga-Pflücker, An overview of the intrathymic intricacies of T cell development. *J. Immunol.* **192**, 4017–4023 (2014).
12. M. A. Yui, E. V. Rothenberg, Developmental gene networks: A triathlon on the course to T cell identity. *Nat. Rev. Immunol.* **14**, 529–545 (2014).
13. T. K. Starr, S. C. Jameson, K. A. Hogquist, Positive and negative selection of T cells. *Annu. Rev. Immunol.* **21**, 139–176 (2003).
14. I. Aifantis *et al.*, The E delta enhancer controls the generation of CD4- CD8- alphabetaTCR-expressing T cells that can give rise to different lineages of alphabeta T cells. *J. Exp. Med.* **203**, 1543–1550 (2006).
15. C. Trigueros *et al.*, Identification of a late stage of small noncycling pTalpha- pre-T cells as immediate precursors of T cell receptor α/β+ thymocytes. *J. Exp. Med.* **188**, 1401–1412 (1998).
16. M. A. Berger *et al.*, Subunit composition of pre-T cell receptor complexes expressed by primary thymocytes: CD3 delta is physically associated but not functionally required. *J. Exp. Med.* **186**, 1461–1467 (1997).
17. V. P. Dave *et al.*, CD3 delta deficiency arrests development of the alpha beta but not the gamma delta T cell lineage. *EMBO J.* **16**, 1360–1370 (1997).
18. S. M. Hayes, P. E. Love, Distinct structure and signaling potential of the gamma delta TCR complex. *Immunity* **16**, 827–838 (2002).
19. G. Awong *et al.*, Characterization in vitro and engraftment potential in vivo of human progenitor T cells generated from hematopoietic stem cells. *Blood* **114**, 972–982 (2009).
20. A.-S. Wiekmeijer *et al.*, Identification of checkpoints in human T-cell development using severe combined immunodeficiency stem cells. *J. Allergy Clin. Immunol.* **137**, 517–526.e3 (2016).
21. T. Taghon *et al.*, Notch signaling is required for proliferation but not for differentiation at a well-defined β-selection checkpoint during human T-cell development. *Blood* **113**, 3254–3263 (2009).
22. K. Canté-Barrett *et al.*, Loss of CD44^{dim} expression from early progenitor cells marks T-cell lineage commitment in the human thymus. *Front. Immunol.* **8**, 32 (2017).
23. K. A. Hogquist *et al.*, T cell receptor antagonist peptides induce positive selection. *Cell* **76**, 17–27 (1994).
24. A. E. Moran *et al.*, T cell receptor signal strength in T_{reg} and iNKT cell development demonstrated by a novel fluorescent reporter mouse. *J. Exp. Med.* **208**, 1279–1289 (2011).
25. J. Zikherman, R. Parameswaran, A. Weiss, Endogenous antigen tunes the responsiveness of naive B cells but not T cells. *Nature* **489**, 160–164 (2012).
26. M. A. Daniels *et al.*, Thymic selection threshold defined by compartmentalization of Ras/MAPK signalling. *Nature* **444**, 724–729 (2006).
27. T. K. Teague *et al.*, CD28 expression redefines thymocyte development during the pre-T to DP transition. *Int. Immunol.* **22**, 387–397 (2010).
28. C. J. Guidos, I. L. Weissman, B. Adkins, Developmental potential of CD4-8- thymocytes. Peripheral progeny include mature CD4-8- T cells bearing alpha beta T cell receptor. *J. Immunol.* **142**, 3773–3780 (1989).
29. A. G. Schrum, L. A. Turka, E. Palmer, Surface T-cell antigen receptor expression and availability for long-term antigenic signaling. *Immunol. Rev.* **196**, 7–24 (2003).
30. N. Kang-Decker *et al.*, Loss of CBP causes T cell lymphomagenesis in synergy with p27Kip1 insufficiency. *Cancer Cell* **5**, 177–189 (2004).
31. M. Mingueneau *et al.*; Immunological Genome Consortium, The transcriptional landscape of αβ T cell differentiation. *Nat. Immunol.* **14**, 619–632 (2013).
32. L. A. Turka *et al.*, Thymocyte expression of RAG-1 and RAG-2: Termination by T cell receptor cross-linking. *Science* **253**, 778–781 (1991).
33. D. M. Krupke *et al.*, The mouse tumor biology database: A comprehensive resource for mouse models of human cancer. *Cancer Res.* **77**, e67–e70 (2017).
34. S. C. Neier *et al.*, The early proximal αβ TCR signalosome specifies thymic selection outcome through a quantitative protein interaction network. *Sci. Immunol.* **4**, eaal2201 (2019).
35. M. L. Oliveira *et al.*, From the outside, from within: Biological and therapeutic relevance of signal transduction in T-cell acute lymphoblastic leukemia. *Cell. Signal.* **38**, 10–25 (2017).
36. T. Girardi, C. Vicente, J. Cools, K. De Keersmaecker, The genetics and molecular biology of T-ALL. *Blood* **129**, 1113–1123 (2017).
37. J. De Bie *et al.*, Single-cell sequencing reveals the origin and the order of mutation acquisition in T-cell acute lymphoblastic leukemia. *Leukemia* **32**, 1358–1369 (2018).
38. M. R. Mansour *et al.*, Notch-1 mutations are secondary events in some patients with T-cell acute lymphoblastic leukemia. *Clin. Cancer Res.* **13**, 6964–6969 (2007).
39. M. A. Daniels, K. A. Hogquist, S. C. Jameson, Sweet 'n' sour: The impact of differential glycosylation on T cell responses. *Nat. Immunol.* **3**, 903–910 (2002).
40. D. Gil, A. G. Schrum, M. A. Daniels, E. Palmer, A role for CD8 in the developmental tuning of antigen recognition and CD3 conformational change. *J. Immunol.* **180**, 3900–3909 (2008).
41. Q. Leng, Q. Ge, T. Nguyen, H. N. Eisen, J. Chen, Stage-dependent reactivity of thymocytes to self-peptide–MHC complexes. *Proc. Natl. Acad. Sci. U.S.A.* **104**, 5038–5043 (2007).
42. L. Strzadala, A. Miazek, J. Matuszyk, P. Kisielow, Role of thymic selection in the development of thymic lymphomas in TCR transgenic mice. *Int. Immunol.* **9**, 127–138 (1997).
43. T. Serwold, K. Hochedlinger, M. A. Inlay, R. Jaenisch, I. L. Weissman, Early TCR expression and aberrant T cell development in mice with endogenous prerearranged T cell receptor genes. *J. Immunol.* **179**, 928–938 (2007).
44. A. Wilson, H. R. MacDonald, Expression of genes encoding the pre-TCR and CD3 complex during thymus development. *Int. Immunol.* **7**, 1659–1664 (1995).
45. B. Wang *et al.*, T lymphocyte development in the absence of CD3 epsilon or CD3 gamma delta epsilon zeta. *J. Immunol.* **162**, 88–94 (1999).
46. T. Serwold *et al.*, T-cell receptor-driven lymphomagenesis in mice derived from a reprogrammed T cell. *Proc. Natl. Acad. Sci. U.S.A.* **107**, 18939–18943 (2010).
47. J. Buer, I. Aifantis, J. P. DiSanto, H. J. Fehling, H. von Boehmer, Role of different T cell receptors in the development of pre-T cells. *J. Exp. Med.* **185**, 1541–1547 (1997).
48. M. C. Haks *et al.*, Low activation threshold as a mechanism for ligand-independent signaling in pre-T cells. *J. Immunol.* **170**, 2853–2861 (2003).
49. Y. Cui *et al.*, Thymic expression of a T-cell receptor targeting a tumor-associated antigen coexpressed in the thymus induces T-ALL. *Blood* **125**, 2958–2967 (2015).
50. H. C. O'Neill, M. S. McGrath, J. P. Allison, I. L. Weissman, A subset of T cell receptors associated with L3T4 molecules mediates C6VL leukemia cell binding of its cognate retrovirus. *Cell* **49**, 143–151 (1987).
51. H. C. O'Neill, Interleukin-2 and antibody to the T cell receptor regulate proliferation of a radiation leukemia virus-transformed T cell lymphoma. *Leukemia* **2**, 108–114 (1988).
52. H. C. O'Neill, Preferential expression of a common T cell receptor structure by T cells induced to proliferate in vitro with a murine retrovirus. *Cell. Immunol.* **136**, 54–61 (1991).
53. H. C. O'Neill, Radiation leukemia virus-induced T-cell lymphomas with common T-cell receptor variable region structure and similar binding specificity for retrovirus. *Leukemia* **5**, 921–927 (1991).

54. R. Fulton, D. Forrest, R. McFarlane, D. Onions, J. C. Neil, Retroviral transduction of T-cell antigen receptor beta-chain and myc genes. *Nature* **326**, 190–194 (1987).
55. G. Webster, D. E. Onions, J. C. Neil, E. R. Cameron, Skewed T-cell receptor Vbeta8.2 expression in transgenic CD2-myc induced thymic lymphoma: A role for antigen stimulation in tumour development? *Br. J. Cancer* **76**, 739–746 (1997).
56. E. R. Cameron *et al.*, Apparent bypass of negative selection in CD8+ tumours in CD2-myc transgenic mice. *Br. J. Cancer* **73**, 13–17 (1996).
57. L. Madsen *et al.*, Mice lacking all conventional MHC class II genes. *Proc. Natl. Acad. Sci. U.S.A.* **96**, 10338–10343 (1999).
58. R. J. Stiles, A. G. Schrum, D. Gil, A co-housing strategy to improve fecundity of mice in timed matings. *Lab Anim. (NY)* **42**, 62–65 (2013).
59. N. Kotecha, P. O. Krutzik, J. M. Irish, Web-based analysis and publication of flow cytometry experiments. *Curr. Protoc. Cytom.* **Chapter 10(1)**, Unit10.17–10.17.24 (2010).
60. J. O'Neil *et al.*, Activating Notch1 mutations in mouse models of T-ALL. *Blood* **107**, 781–785 (2006).
61. B. S. Carvalho, R. A. Irizarry, A framework for oligonucleotide microarray preprocessing. *Bioinformatics* **26**, 2363–2367 (2010).
62. H. Shimodaira, Approximately unbiased tests of regions using multistep-multiscale bootstrap resampling. *Ann. Stat.* **32**, 2616–2641 (2004).
63. R. Suzuki, H. Shimodaira, Pvclust: An R package for assessing the uncertainty in hierarchical clustering. *Bioinformatics* **22**, 1540–1542 (2006).
64. S. L. Johnston, P. J. Wettstein, T cell receptor diversity in CTLs specific for the CTT-1 and CTT-2 minor histocompatibility antigens. *J. Immunol.* **159**, 2606–2615 (1997).
65. Laffey, K.G, Expression Data of murine T-ALL OT-1 (Tot-1si) with early expression of mature alphabeta T CR. Gene Expression Omnibus. https://www.ncbi.nlm.nih.gov/geo/query/acc.cgi?acc=GSE180556. Accessed July 21, 2021.